Available online at www.sciencedirect.com
SCIENCE DIRECT
Polymer 47 (2006) 5108–5116
polymer
www.elsevier.com/locate/polymer

Effect of oscillatory shear on the interfacial morphology of a reactive bilayer polymer system

Hwang Yong Kim, Dong Hyun Lee, Jin Kon Kim *

National Creative Research Center for Block Copolymer Self-Assembly, Department of Chemical Engineering and Polymer Research Institute, Pohang University of Science and Technology, Kyungbuk 790-784, South Korea

Received 4 February 2006; received in revised form 8 May 2006; accepted 9 May 2006
Available online 5 June 2006

Abstract

We investigated, via atomic force microscopy and transmission electron microscopy, the effect of oscillatory shearing amplitude (γ_0) and frequency (ω) on the interfacial morphology of a reactive bilayer polymer system composed of end-functionalized polystyrene with carboxylic acid (PS-mCOOH) and poly(methyl methacrylate-*ran*-glycidylmethacrylate) (PMMA–GMA). It has been observed that in the absence of oscillatory shearing (or at very small values of γ_0 and ω), the roughness of the interface increased with reaction period, while at large values of γ_0 and ω it became less than that observed in the absence of oscillatory shearing. This observation may be attributable to the possibility that oscillatory shearing might have hindered the diffusion of polymer chains, which are located away from the interface, to the interface of the layers. However, the effect of γ_0 and ω on the roughness of the interface of (PS-mCOOH)/(PMMA–GMA) bilayer is found to be quite different. Specifically, when a large γ_0 was first applied to the bilayer, followed by application of a low γ_0, the reactive polymer chains diffused into the interface of the (PS-mCOOH)/(PMMA–GMA) bilayer; and then the roughness of the interface increased. However, when a high ω of oscillatory shear flow was first applied to a specimen, followed by application of a low ω of oscillatory shear flow to the same specimen, a relatively low degree of roughness of the interface was observed. This is attributable to the fact that the oscillatory shear with a large ω generated a multilayer microstructure consisting of PS and PMMA layers, which apparently played the role of an obstacle (or diffusion barrier) that hindered the diffusion of both reactive polymer chains to the interface for chemical reactions.

Keywords: Shear force; Interfacial thickness; Reactive blending

1. Introduction

Reactive blending of two or more immiscible polymers with in-situ formation of block or graft copolymer has been employed for developing new materials with desirable physical and mechanical properties, and has extensively been investigated by many research groups [1–6]. Most studies on reactive blending have focused on the final morphology of polymer blends, which determines mechanical properties [7–11]. Among the many factors that influence the final morphology in a reactive polymer blend system, the amount of in-situ formed diblock (or graft) copolymers (or reaction kinetics) and the applied shearing force become very important.

Recently, many studies have focused on investigating the effect of reaction kinetics on the interfacial morphology of reactive bilayer system using transmission electron microscopy (TEM), atomic force microscopy (AFM), forward recoil spectrometry (FRES), and dynamic secondary ion mass spectrometry [12–24]. It should be noted that the interfacial morphology of reactive bilayer system depends on the reaction kinetics of two reactive polymers, the position of the functional group in a reactive polymer chain, and the molecular weight of the polymers.

On the other hand, many reactive polymer blends have been prepared using commercially available compounding machines, such as continuous extruders or batch-type internal mixers [25–27]. However, an analysis of flow of two reactive polymers in a compounding machine is very difficult in general. Also, there are few studies reported on the effect of shear force applied on reactive bilayer polymer systems having a well-defined interface. To understand the effect of shearing force on the reaction kinetics associated with a reactive bilayer polymer system and the development of the interfacial morphology during the reaction, the flow should be well-characterized.

* Corresponding author. Tel.: +82 54 279 2276; fax: +82 54 279 8298.
E-mail address: jkkim@postech.ac.kr (J.K. Kim).

0032-3861/$ - see front matter © 2006 Elsevier Ltd. All rights reserved.
doi:10.1016/j.polymer.2006.05.019

In a previous paper [28], we reported that the interfacial reaction and variations of the extent of the roughness of the interface in a bilayer polymer system with reaction period and temperature could be monitored using rheological measurements. As oscillatory shear rheometry can provide controlled shear force on a specimen, the roughness of the interface of a reactive bilayer polymer system can be readily monitored under various shearing conditions. In this study, we have investigated the effect of oscillatory shear on the interfacial morphology of a reactive bilayer polymer system composed of end-functionalized polystyrene with carboxylic acid (PS-mCOOH) and poly(methyl methacrylate-*ran*-glycidylmethacrylate) (PMMA–GMA). The reaction between the carboxylic acid in PS-mCOOH and the epoxy groups in PMMA–GMA occurs easily at elevated temperatures [29–33], giving rise to in-situ formation of PMMA-*graft*-PS copolymers. We have found that at low strain amplitude (γ_0) and angular frequency (ω) during oscillatory shearing flow, the morphological development near the interface of the (PS-mCOOH)/(PMMA–GMA) bilayer system was essentially the same as that in the absence of oscillatory shearing (i.e. under quiescent conditions), whereas at large γ_0 or ω, the development of interfacial morphology was significantly different. In this paper, we summarize the results of our investigation.

2. Experimental

2.1. Materials and sample preparation

An end-functionalized polystyrene with carboxylic acid group, PS-mCOOH was purchased from Aldrich Chem. Co. We synthesized via free radical polymerization, a poly(methyl methacrylate-*ran*-glycidylmethacrylate) (PMMA–GMA). The molecular characteristics of the polymers are summarized in Table 1. We prepared a thin sheet of each polymer, PS-mCOOH and PMMA–GMA, using compression molding on Si-wafer to obtain smooth surfaces of the sheets, and then we annealed them at 130 °C for 24 h. The thickness of each sheet was 0.3 mm. The sheet of PS-mCOOH was placed on the top of the PMMA–GMA sheet.

2.2. Rheological measurements

After two layers of PS-mCOOH and PMMA–GMA were placed inside the 25-mm parallel-plate fixture of a rheometer (Advanced Rheometric Expansion System, TA Instruments) at 180 °C under a nitrogen atmosphere, variations of dynamic storage modulus (G') and dynamic loss modulus (G'') were monitored with time at fixed values of strain amplitude (γ_0) ranging from 0.005 to 0.5 and angular frequency (ω), enabling us to calculate the absolute values of complex viscosity ($|\eta^*|$) using the definition, $|\eta^*| = [(G'/\omega)^2 + (G''/\omega)^2]^{1/2}$. Also, values of G' and G'' were measured as functions of ω from 0.1 to 100 rad/s for two neat polymers PS-mCOOH and PMMA–GMA at 180 °C, for which a fixed strain of 0.005 was used to ensure that measurements were taken well within the linear viscoelastic range of the materials investigated. Data acquisition was accomplished with the aid of a microcomputer interfaced with the rheometer. The temperature control was satisfactory to within ±1 °C. All rheological measurements were conducted using a 200 FRTN1 transducer with a lower limit of 0.08 g cm.

Table 1
Molecular characteristics of polymers employed in this study

Samples	M_w (g/mol)	M_w/M_n	η_0 at 180 °C (Pa s)	Function-ality
PS-mCOOH	135,000	1.13	8×10^3	1
PMMA–GMA	115,500	1.7	2.5×10^5	12.5

2.3. Determination of interfacial thickness of interfacial morphology

To investigate variations of interfacial morphology with time for the (PS-mCOOH)/(PMMA–GMA) bilayer system after a predetermined period of reaction time, the specimen was removed from the parallel-plate fixture and then quenched in ice water. Subsequently, the PS layer was completely removed by selectively dissolving solvent of cyclohexane at 40 °C for 35 h. The morphology of the interface was obtained by atomic force microscopy (AFM) (Digital Instrument; D3000) with silicon nitride tips on cantilevers (Nanoprobe) in the tapping mode. The root-mean square (rms) roughness of the interface (δ), defined by $(\sum_i (h_i - \bar{h})^2/n^{1/2}$ with h_i being the height of a particular position, $\bar{h}$ being the average height, and n being the total number of measurement positions, was calculated by the software (Nanoscope) provided by Digital Instrument. The morphology of the cross-section of the bilayer specimens was examined using a transmission electron microscope (Hitachi; 7600) operated at 120 kV. The PS phase of specimens was stained with ruthenium tetroxide (RuO_4) for 15 min, which made the PS phase look dark in the images of transmission electron microscopy (TEM).

3. Results and discussion

Fig. 1 describes variations of $|\eta^*|$ of the (PS-mCOOH)/(PMMA–GMA) bilayer with reaction time at $\gamma_0 = 0.005$ and $\omega = 0.1$ rad/s. During these experiments we learned that variation of $|\eta^*|$ with reaction time was essentially independent of γ_0 for small values of γ_0 (<0.005). Three different regimes are clearly seen in Fig. 1, as also described in our previous paper [28]. At stage I, the sharp interface begins to undulate, because PMMA-*graft*-PS copolymers are formed from the chemical reaction between PS-mCOOH and PMMA–GMA at the interface. The slope of the plots of $|\eta^*|$ versus reaction time at stage I is related to reaction kinetics [28]. At stage II, the $|\eta^*|$ does not increase with reaction time. This is because the reactive polymer chain ends could not diffuse through the densely-packed graft copolymer layer that was formed at stage I. At the final stage III, the reactive polymer chains penetrate again into the densely-packed graft copolymer layers and then undergo further chemical reactions. The interfacial

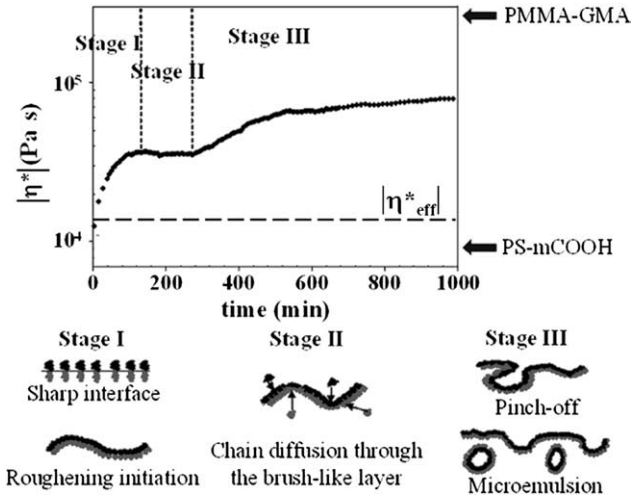

Fig. 1. Plot of $|\eta^*|$ at 180 °C versus time for (PS-mCOOH)/(PMMA–GMA) bilayer and schematic describing variations of interfacial morphology. The dashed line is $|\eta^*_{eff}|$ predicted by Eq. (1).

morphologies corresponding to each of the three stages are given schematically in the lower part of Fig. 1.

Referring to Fig. 1, at first glance the rather large increase in $|\eta^*|$ observed for the (PS-mCOOH)/(PMMA–GMA) reactive bilayer may seem strange. It is noted that $|\eta^*|$ for a polymer bilayer is often given by a simple inverse relationship between the component viscosity and volume fraction of the bilayer [34,35]

$$\frac{1}{\eta_{\text{eff}}} = \frac{\phi_1}{\eta_1} + \frac{\phi_2}{\eta_2} \tag{1}$$

where η_{eff}, η_1 and η_2 denote the viscosities of the bilayer and components 1 and 2, respectively, and ϕ_1 and ϕ_2 denote the volume fractions of layers 1 and 2, respectively. The predicted $|\eta^*|$ by Eq. (1) is given as a dashed line in Fig. 1, which is very small compared with the measure one at 16 h.

However, we do not believe that the use of Eq. (1) or its variations can explain our experimental results for the following reasons. This is because the prediction by Eq. (1) is only valid before the reaction (or at very short reaction times) where the interface between two layers is very small and flat. But, as the reaction proceeds, the interface generated due to chemical reactions between the carboxylic acid group at the chain end of PS-mCOOH and the epoxy groups in PMMA–GMA becomes roughened [28]. This roughened interface would cause the additional friction against the flow near the interface, which increase the viscosity. Also, the interphase consists of PMMA-*graft*-PS copolymers, the strength of which would be much greater than that of the interphase formed strictly from interdiffusion in the absence of chemical reaction. Therefore, we are of the opinion that these two effects would be primarily responsible for the very large values of $|\eta^*|$ observed at stage III depicted in Fig. 1. It is worth mentioning at this juncture that very recently, a large increase in $|\eta^*|$ has been reported by Yu et al. [36] who employed a reactive bilayer composed of polyamide 6 and poly(styrene-*co*-maleic anhydride).

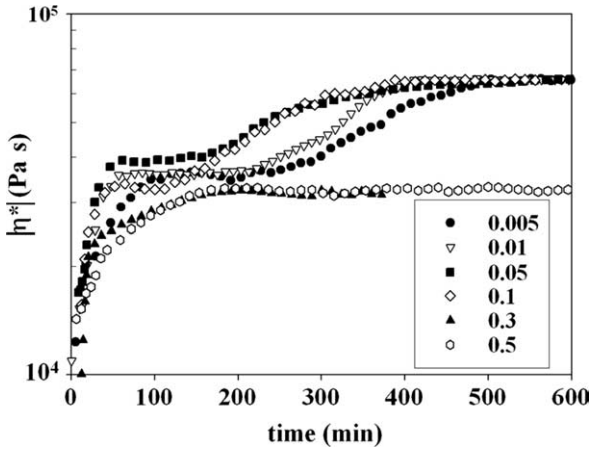

Fig. 2. Plot of $|\eta^*|$ at $\omega = 0.1$ rad/s and 180 °C versus time for (PS-mCOOH)/(PMMA–GMA) bilayer at various strain amplitudes.

Fig. 2 gives variations of $|\eta^*|$ of (PS-mCOOH)/(PMMA–GMA) bilayer system with reaction time at 180 °C and $\omega = 0.1$ rad/s for different values of γ_0. With increasing γ_0 from 0.005 to 0.05, the slope of the plots of $|\eta^*|$ versus reaction time at stage I becomes larger, suggesting that the time required for the PMMA-*graft*-PS copolymer to cover a single layer at the interface becomes shortened. Also, the lag time for the polymer chains to diffuse across the interface at stage II (thus, the inception of stage III) becomes shortened with increasing γ_0. This is attributed to the fact that the shearing force helps to generate easily new vacant sites near the interface, where the reactive chains could diffuse and react to form additional copolymers. But, the final value of $|\eta^*|$ after a very long period of reaction time (for instance, 10 h) is almost the same for $\gamma_0 < 0.05$. This observation indicates that a small-amplitude oscillatory shearing does not contribute to the generation of additional interfacial areas even after a long period of reaction times.

On the other hand, referring to Fig. 2, variations of $|\eta^*|$ with reaction time for larger values of γ_0 (> 0.3) are quite different from those for low values of γ_0 (< 0.3). Notice in Fig. 2 that for $\gamma_0 > 0.3$, $|\eta^*|$ increases for a short period of reaction time because two polymer chains located near the interface undergo chemical reactions easily, but stage III is not observed even for a very long period (10 h) of reaction time. This observation suggests that the oscillatory shearing force with large γ_0 might hinder further chemical reactions even for a long period of reaction at stage III. Namely, with increasing shearing force, the interdiffusion of both polymer chains in the direction perpendicular to the interface might be significantly reduced. Previously, Kim and Han [37] have shown that the diffusion coefficients of PMMA and poly(vinylidene fluoride) perpendicular to the flow direction, when they were coextruded through a cylindrical tube under steady-state shear flow, were significantly lower than the bulk diffusion coefficients. Although the present investigation was not conducted under steady-state shear conditions, polymer chains would be stretched toward the shear direction, which would then hinder

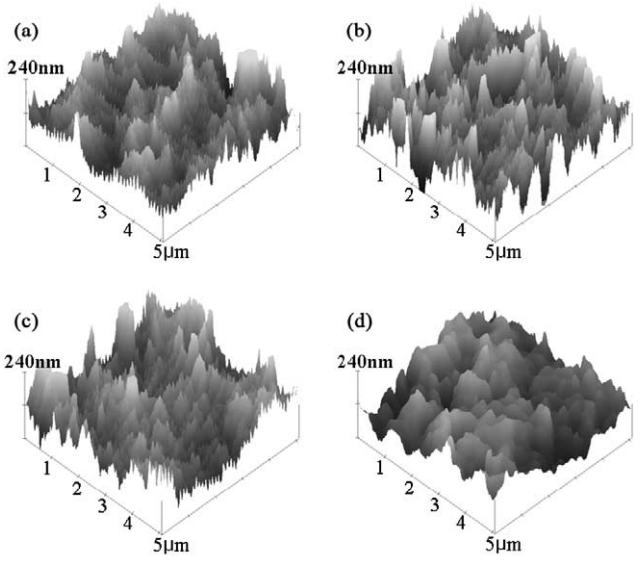

Fig. 3. AFM images describing the variation of undulations of the interface of specimens that were subjected to chemical reaction for a period of 10 h at various strain amplitudes (γ_0): (a) $\gamma_0=0.005$ (δ=ca. 180 nm), (b) $\gamma_0=0.01$ (δ=ca. 180 nm), (c) $\gamma_0=0.05$ (δ=ca. 180 nm), and (d) $\gamma_0=0.5$ (δ=ca. 40 nm).

the diffusion of the polymer chains perpendicular to the shear direction.

Since an increase in $|\eta^*|$ after a long period of reaction time at stage III is directly related to the large undulations of interface [28], the interfacial morphology at the end of reaction period of 10 h for $\gamma_0=0.5$ would be quite different from that for smaller values of γ_0. Fig. 3 gives AFM images describing interface undulations at the end of reaction period for 10 h for four different values of γ_0. The following observations are worth noting in Fig. 3. For $\gamma_0<0.05$, δ is the same (ca. 180 nm), but for $\gamma_0=0.5$ it is very small (ca. 40 nm), which is almost the same as that observed at the end of stage I (or the beginning of stage II). Therefore, we conclude that further chemical reaction did not occur after stage I for large values of γ_0 (say 0.5). This observation seems to suggest that although the reactive polymer chains near the interface undergo chemical reactions for earlier reaction period, the barrier to the diffusion of reactive polymer chains might be very large for large values of γ_0, hindering the penetration of the reactive polymer chains through the layer of densely-packed graft copolymers that were formed at stage I.

It would be interesting to know whether this kind of diffusion barrier could be removed when large γ_0 was relaxed. To test such a possibility, we conducted a step-down shear amplitude experiment, namely we first applied $\gamma_0=0.5$ for 8 h, and then $\gamma_0=0.005$. As shown in Fig. 4, when $\gamma_0=0.005$ was applied, the $|\eta^*|$ started to increase again with reaction time, and then leveled off at $|\eta^*|=7.5\times10^4$ Pa s, which is virtually the same as that obtained for $\gamma_0<0.3$ (Fig. 2). Furthermore, δ increased from ca. 40 to 180 nm, as shown in the AFM images given in Fig. 4. Therefore, we conclude that the diffusion barrier generated under large oscillatory shearing forces for large values of γ_0 can be removed completely when γ_0 was decreased below a certain critical value.

Fig. 5 describes the results of frequency sweep experiments for two homopolymers, PS-mCOOH and PMMA–GMA, at 180 °C. The cross-over frequency (ω_c), at which $G'=G''$ holds, is 12.0 rad/s for PS-mCOOH and 0.34 rad/s for PMMA–GMA, while values of G' and G'' at ω_c are very similar (ca. 3×10^4 Pa) for the two homopolymers.

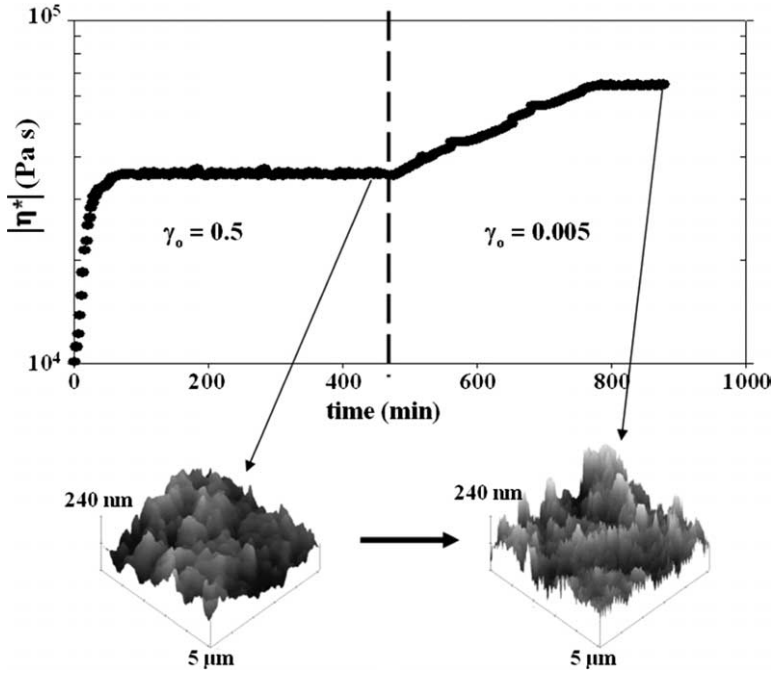

Fig. 4. Variations of $|\eta^*|$ at $\omega=0.1$ rad/s and 180 °C with time after a step-decrease of strain amplitude from $\gamma_0=0.5$ (on the left side of the dashed vertical line) to $\gamma_0=0.005$ (on the right side of the dashed vertical line). During a step-decrease in γ_0, δ has increased from ca. 40 to 180 nm.

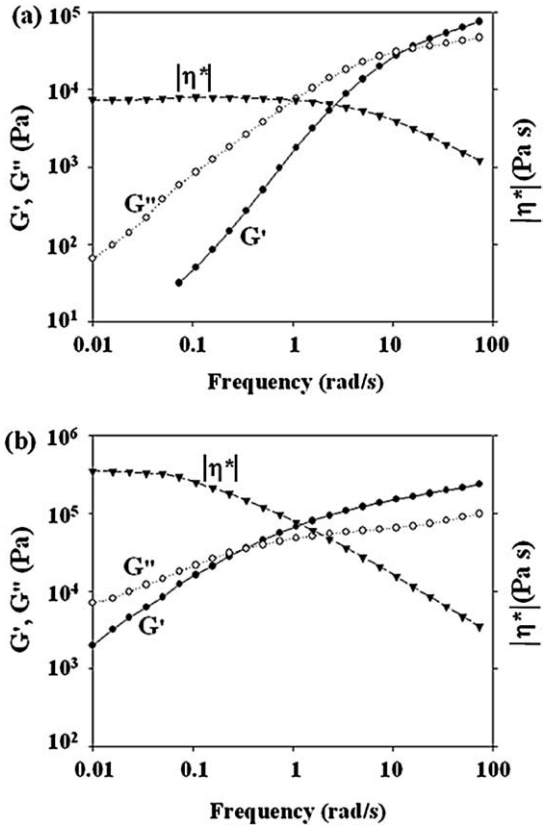

Fig. 5. Plots of G', G'' and $|\eta^*|$ versus ω at 180 °C: (a) PS-mCOOH and (b) PMMA–GMA.

Fig. 6 gives variations of $|\eta^*|$ with reaction time at 180 °C for various values of ω (0.1–100 rad/s) at $\gamma_0 = 0.005$. For $\omega <$ 5 rad/s, the reaction times corresponding to the beginning of stage II and stage III decreased with increasing ω, as shown in Fig. 6(a) and (b). We found that δ after a reaction period of 10 h at $\omega = 5$ rad/s was ca. 180 nm, although AFM image is not shown for the reason of limit space available, indicating that stage III was achieved under this condition even though stage II is barely seen. Very interestingly, variations of $|\eta^*|$ with reaction time at $\omega = 10$ and 100 rad/s are quite different from those observed at lower values of ω. Namely, at $\omega = 10$ and 100 rad/s the $|\eta^*|$ increases up to 30 min of reaction time, and then decreases approaching a constant value. This observation has not been made for the same reactive bilayer system even for larger values of γ_0 at smaller values of ω. In fact, the value of $|\eta^*|$ levels off at a constant value with increasing reaction time (Figs. 2 and 4).

Fig. 7 gives AFM images of the interface of the reactive bilayer system subjected to chemical reactions for 10 h at 180 °C for four different values of ω. For the bilayer system subjected to chemical reaction at $\omega < 5$ rad/s, δ is ca. 180 nm. However, for the bilayer system subjected to chemical reaction at $\omega = 100$ rad/s, δ corresponding to the reaction time where a maximum in $|\eta^*|$ is observed is ca. 40 nm, and that corresponding to the reaction time where steady-state value of $|\eta^*|$ is observed is ca. 20 nm. This clearly indicates that at $\omega = 100$ rad/s the extent of interfacial roughness decreases at longer periods of reaction time.

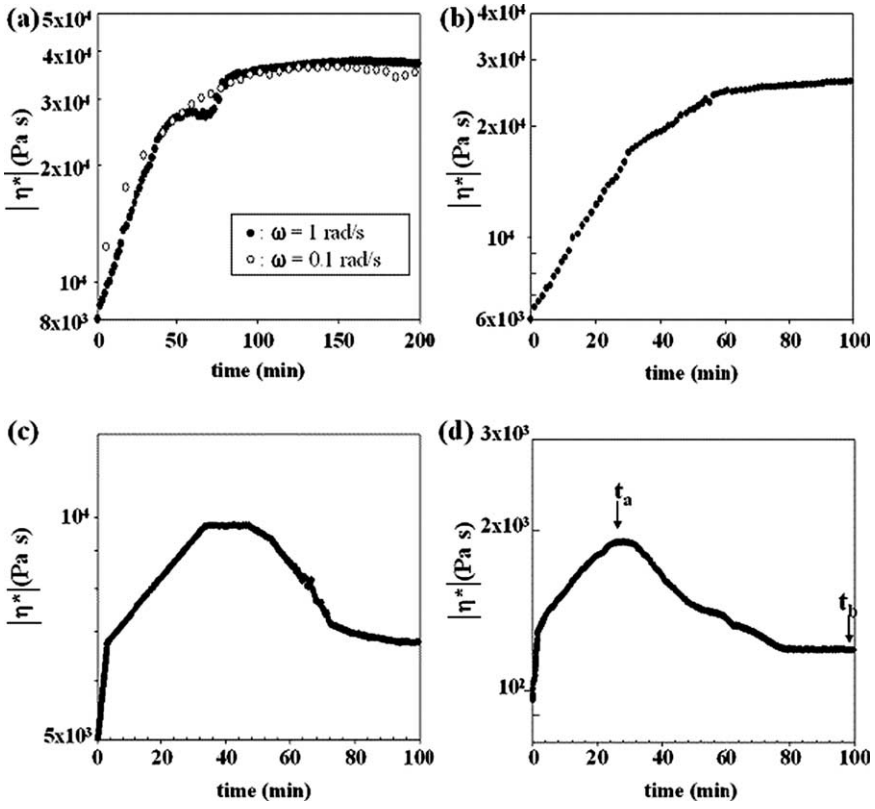

Fig. 6. Plot of $|\eta^*|$ at 180 °C versus time for (PS-mCOOH)/(PMMA–GMA) bilayer at various values of angular frequency (ω). (a) 0.1 and 1 rad/s, (b) 5 rad/s, (c) 10 rad/s and (d) 100 rad/s.

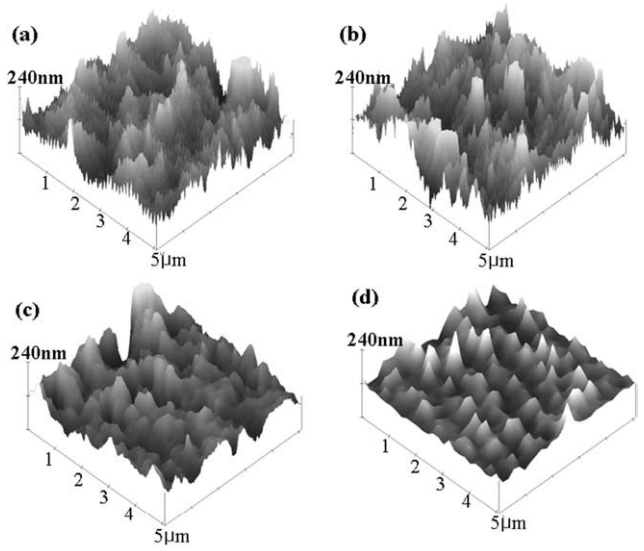

Fig. 7. AFM images of the specimens subjected to chemical reaction for different values of angular frequency (ω): (a) after 10 h of reaction at $\omega = 0.1$ rad/s (δ = ca. 180 nm), (b) after 10 h of reaction at $\omega = 1$ rad/s (δ = ca. 180 nm), (c) after 25 min of reaction at $\omega = 10$ rad/s (δ = ca. 40 nm), and (d) after 100 min at $\omega = 100$ rad/s (δ = ca. 20 nm).

It is of interest to examine whether the low value of $|\eta^*|$ (or δ) obtained at a high ω increases again when ω is lowered. As shown in Fig. 4, the hindered diffusion of homopolymer chains at large γ_0 was recovered when γ_0 was decreased. Fig. 8 gives variations of $|\eta^*|$ with reaction time after ω was decreased stepwise from 100 to 0.1 rad/s. Interestingly, $|\eta^*|$ did not increase with a further increase of reaction period, except for an initial increase in $|\eta^*|$. This initial increase in $|\eta^*|$ is because of the difference in the $|\eta^*|$ between 0.1 and 100 rad/s for each reactive homopolymer (PS-mCOOH and PMMA–GMA), as shown in Fig. 5. We have also found that δ was the same (ca. 20 nm) even when ω was lowered. This observation suggests that stage III was not achieved once the reactive

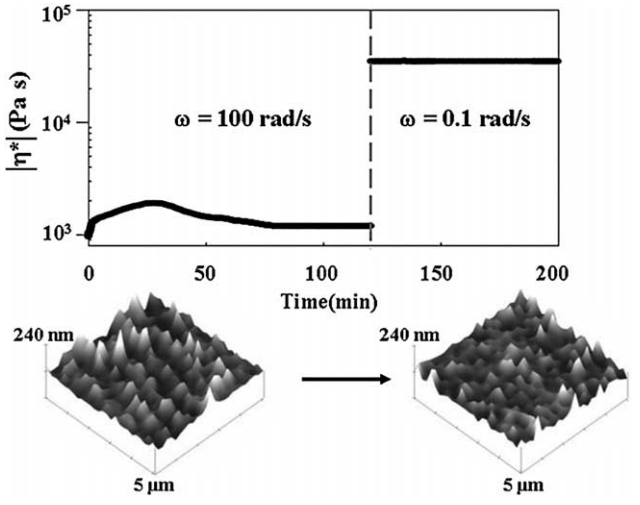

Fig. 8. Variations of $|\eta^*|$ at 180 °C with time after a step-decrease of angular frequency (ω) from 100 rad/s (on the left side of dotted vertical lime) to 0.1 rad/s (on the right side dotted vertical line). During this step-decrease in ω, the rms roughness of the interface has remained the same (ca. 20 nm).

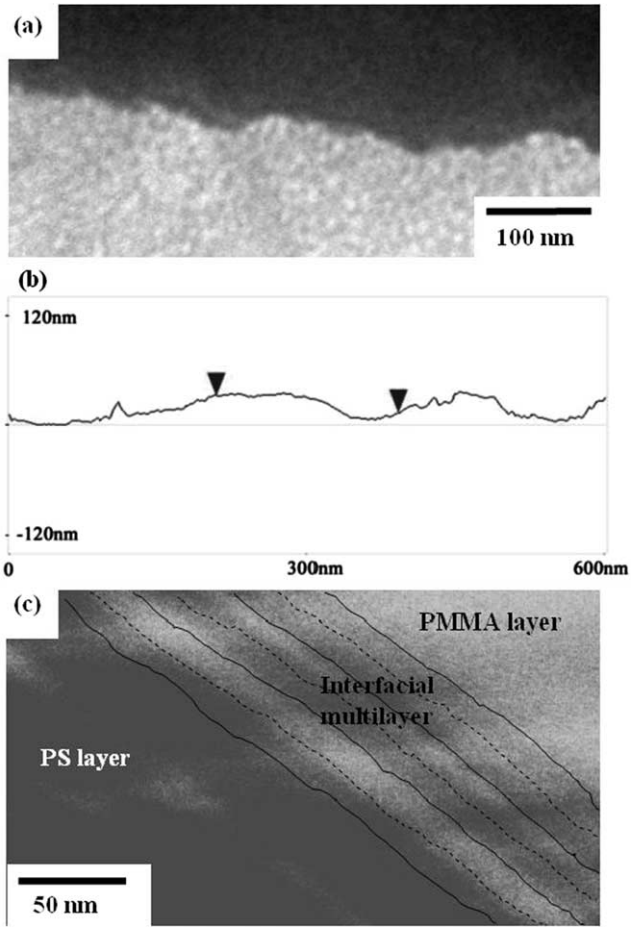

Fig. 9. (a) TEM image and (b) AFM image of a specimen that was subjected to chemical reaction for a period of 25 min at 180 °C and $\omega = 100$ rad/s, and (c) TEM image of a sample that was subjected to chemical reaction for a period of 100 min at 180 °C and $\omega = 100$ rad/s.

bilayer was initially subjected to oscillatory shearing flow at large values of ω. Therefore, the shearing at large values of ω changed the interfacial morphology permanently.

To investigate the interfacial morphology in more detail, TEM images were taken of the cross section of the (PS-mCOOH)/(PMMA–GMA) bilayer. This is because the AFM image gives only the morphology at the outermost part of the interface. Fig. 9 gives TEM images and AFM profile of the bilayer subjected to chemical reaction at $\omega = 100$ rad/s for two different periods (25 and 100 min) of chemical reaction. For a period of reaction of 25 min, only undulated interface between the two layers was observed, and the rms roughness and wavelength of the interface given in Fig. 9(a) are very similar to those obtained by the AFM image given in Fig. 9(b). However, for a period of reaction of 100 min, alternating layers of PS and PMMA indicated by dotted lines were observed in the interface, though imperfect, as shown in Fig. 9(c). The domain spacing (D), which is the sum of one PS and one PMMA layer (indicated by the solid line) is ca. 27 nm. It is of interest to compare the domain spacing of the alternating layers of PS and PMMA with that of PMMA-*graft*-PS copolymer generated from the blends of two reactive homopolymers. For this purpose, PMMA-*graft*-PS copolymer was prepared by

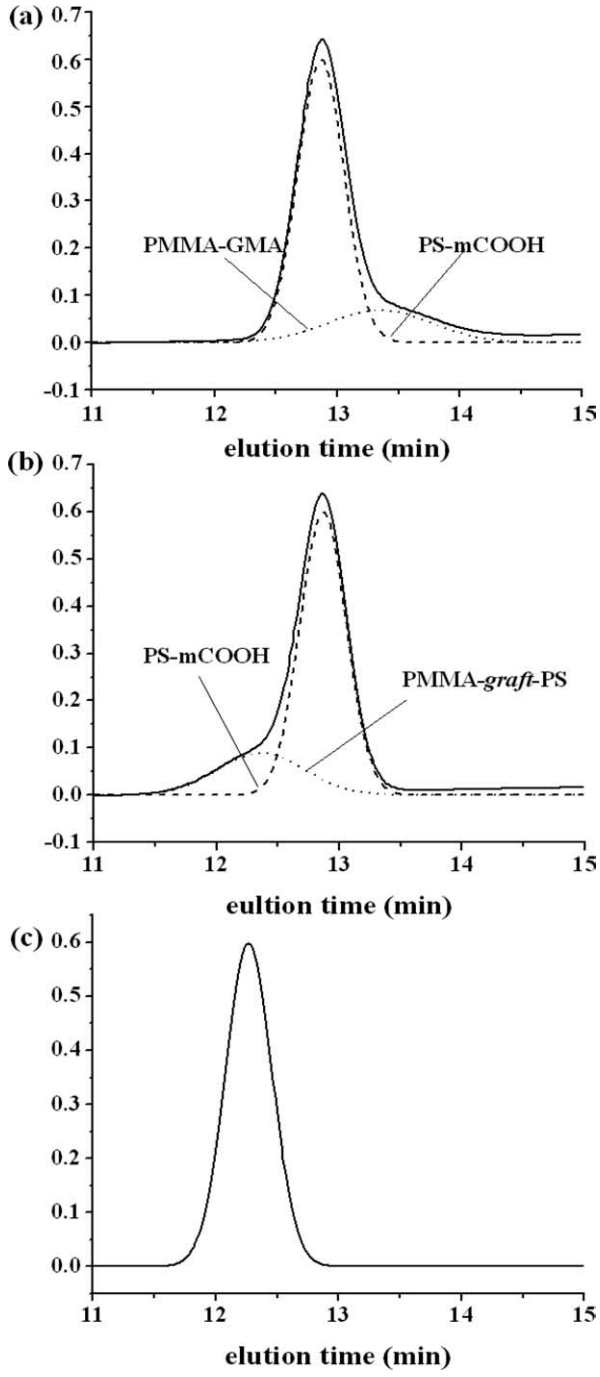

Fig. 10. GPC traces of a mixture of 90/10 (wt/wt) PS-mCOOH and PMMA–GMA (a) before and (b) after the reaction at the interface, and (c) PMMA-*graft*-PS copolymer after removal of unreacted PS-mCOOH. The solid curves represent experimental results and the dashed curves represent deconvolution of GPC traces.

solution blending of 90/10 (wt/wt) PS-mCOOH and PMMA–GMA mixture in toluene at 60 °C for 24 h, followed by precipitation in cylcohexane maintained at 40 °C. Then the powder was filtered and dried at room temperature.

Fig. 10 gives traces of gel permeation chromatography (GPC, Waters Co., 600F) for a mixture of 90/10 (wt/wt) PS-mCOOH and PMMA–GMA (a) before and (b) after the reaction, and (c) PMMA-*graft*-PS copolymer after complete

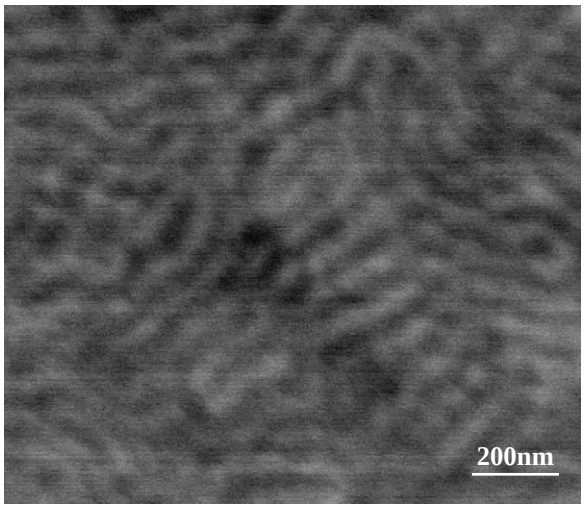

Fig. 11. TEM image for neat PMMA-*graft*-PS copolymer. The PS phase appearing as dark areas was stained with RuO_4.

removal of unreacted PS-mCOOH. It is seen in Fig. 10 that PMMA-*graft*-PS copolymer does not contain any unreacted PMMA–GMA, leading us to conclude that the entire amount of PMMA–GMA added to the reactor has reacted with PS-mCOOH. Fig. 11 gives TEM image of PMMA-*graft*-PS copolymer annealed at 180 °C for 24 h, where lamellar microdomains are clearly seen, although not fully developed. The value of D of the microdomains is ca. 55 nm, which is about twice the value of D that was observed in Fig. 9(c). The above observations lead us to conclude that the microdomain structure of the alternating multilayers observed in Fig. 9(c) must be different from that of PMMA-*graft*-PS copolymer.

It should be mentioned that the extent of undulation at the top (or the bottom) of the interface in the TEM image given in Fig. 9(c) is much smoother than that of the reactive layer obtained at lower values of ω, as shown in Fig. 7(a). The existence of the alternating multilayers that can be observed in Fig. 9(c) indicates that the amount of PMMA-*graft*-PS copolymer formed at higher values of ω is greater than that of the severely undulated interface obtained at lower values of ω in which a single layer was formed. Also, the amount of PMMA-*graft*-PS copolymer formed after reaction for a longer period (say, t_b in Fig. 6(d)) at $\omega = 100$ rad/s should at least be greater than that for a shorter period (say, t_a in Fig. 6(d)). Interestingly, however, values of $|\eta^*|$ for longer reaction periods are lower than those for shorter reaction periods (Fig. 6(d)). Therefore, the extent of increase in $|\eta^*|$ for a reactive bilayer depends much more on the rms roughness of the interface than the amount of the PMMA-*graft*-PS copolymer.

On the basis of the results presented in Figs. 7–9, a schematic describing the variation of the reactive interface with reaction time at high ω is given in Fig. 12. For a short period of reaction time, two reactive polymer chains located near the interface would react for a short period, and thus the rms roughness of the interface is expected to be the same as that obtained at low ω (Fig. 12(a)). However, once a single layer of densely-packed PMMA-*graft*-PS copolymer is formed near the

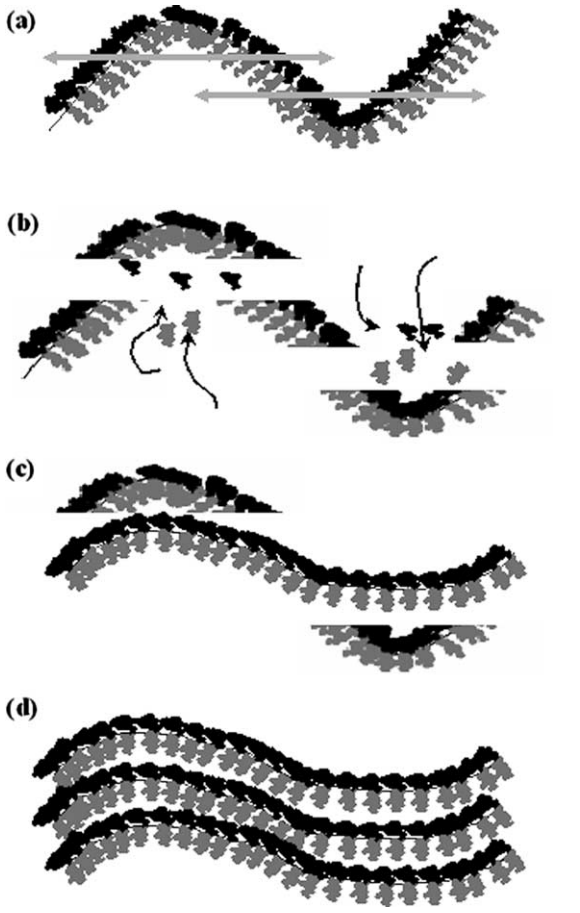

Fig. 12. Schematic describing morphological development near the interface with reaction time at high angular frequencies. (a) Undulated interface, (b) broken interfacial layer at a high angular frequency and further reaction occurs at new vacant site, (c) coexistence of undulated interface and broken copolymer layer, and (d) the formation of a graft copolymer with multilayer microstructure in the interfacial region.

interface, there exists an induction time (or time lag) for the reactive polymer chains to penetrate into the layer of this graft copolymer. However, during this period, the shear force at high ω may break the undulated interface. Then, the reactive polymer chains located away from the interface can penetrate into the interfacial region through the vacant sites formed by the breakup of the interface (Fig. 12(b)), and chemical reactions will take place. Under such a situation, both the undulated interface and the broken layer of PMMA-*graft*-PS copolymer might coexist (Fig. 12(c)). The presence of broken layers of PMMA-*graft*-PS copolymer in the interfacial region is indeed demonstrated by the TEM image given in Fig. 13, after a specimen was subjected to oscillatory shear flow at $\omega =$ 100 rad/s for a period of chemical reaction of 50 min. The thickness of the broken layer of PMMA-*graft*-PS copolymer is found to be ca. 13 nm, which is almost the same as the layer thickness of one PS layer (or one PMMA layer) given in Fig. 9(c). Then, another breakup of PMMA-*graft*-PS copolymer layer located near the interface may occur. Recurrence of such events eventually might have led to the formation of the multilayer structure observed in Fig. 9(c).

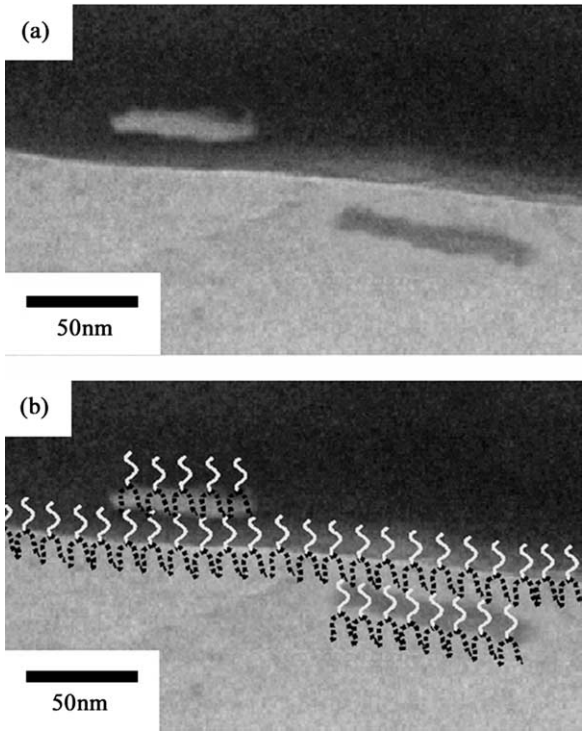

Fig. 13. (a) TEM image for the reactive bilayer for a period of reaction time of 50 min at 180 °C at $\omega = 100$ rad/s. (b) Schematic describing the molecular architecture of graft copolymers in each layer, in which the bright solid line represents PMMA chains and the dark dotted line represents PS chains.

It should be mentioned that the microdomain structure of the multilayer of PMMA-*graft*-PS copolymer in the interfacial region is different from that of neat graft copolymer, where one microdomain consists of two polymer chains of each block having the following sequence A-[BB]-[AA]-[BB]-A, in which – denotes the connectivity between two blocks and the bracket denotes each microdomain. However, each layer in the multilayer structure observed in this study (Fig. 9(c)) consists of only one polymer chain having the following sequence [A]-[B][A]-[B][A]-[B]. In our previous studies [32], we have shown that although PMMA–GMA has 12.5 functional groups of GMA across a PMMA chain, only 1 or 2 PS chains of PS-mCOOH were grafted onto the PMMA–GMA chains. This is illustrated by the schematic given in Fig. 13(b), where PMMA-*graft*-PS copolymer is assumed to have the Y-shaped architecture [28]. We speculate that this kind of multilayer structure (Fig. 12(d)) may act as an obstacle to the reactive polymer chains, which otherwise would diffuse to the interface.

4. Conclusions

In this study, we have investigated the effect of oscillatory shear amplitude and angular frequency on the interfacial morphology of a reactive bilayer composed of PS-mCOOH and PMMA–GMA. We have found that the shear force applied on a specimen during oscillatory shear flow has a significant influence on the extent of interfacial reaction and interfacial morphology. The strain amplitude (γ_0) and angular frequency (ω) were found to help enhance the extent of chemical

reactions at the interface between the two layers and the generation of an interphase, as long as their magnitudes are small. However, at large values of γ_0 and ω, oscillatory shearing is found to inhibit the diffusion of polymer chains to the interface, thus chemical reactions at the interface.

We have found that during oscillatory shear flow, the application of large γ_0 to a specimen generates alternating solidlike layers of (PS-mCOOH)/(PMMA-*graft*-PS) copolymer, which then act as a barrier for the diffusion of reactive polymer chains, which are located away from the interface, to the interface and thus chemical reactions at the interface are restricted. However, when small γ_0 are applied to a specimen subsequent to the application of a large γ_0, chemical reactions take place again at the interface. On the other hand, higher values of ω can break the interface and generate a multilayer of graft copolymer. In this situation, even though a low value of ω was applied again, further reaction did not occur; thus this inhibition becomes permanent obstacle to a further interfacial reactions.

Acknowledgements

This work was supported by the National Creative Research Initiative Program supported by Korea Organization of Science and Engineering Foundation.

References

[1] Ide F, Hasegawa AJ. Appl Polym Sci 1974;18:963.
[2] Xanthos M. Reactive extrusion: principles and practice. New York: Hanser; 1992 [chapter 4].
[3] Pagnoulle C, Korning C, Leemans L, Jérôme R. Macromolecules 2000; 33:6275.
[4] Pagnoulle C, Jérôme R. Macromolecules 2001;34:965. Pagnoulle C, Jérôme R. Polymer 2001;42:1893.
[5] Koulic C, Yin Z, Pagnoulle C, Gilbert B, Jérôme R. Polymer 2001;42: 2947.
[6] Yin Z, Koulic C, Pagnoulle C, Jérôme R. Macromol Chem Phys 2002; 203:2021.
[7] Paul DR, Newman S. Polymer blends, vol. 1. New York: Academic Press; 1978 p. 11, [chapter 1].
[8] Dao KC. Polymer 1984;25:1527.
[9] Charoensirisomboon P, Chiba T, Solomko SI, Inoue T, Weber M. Polymer 1999;40:6803.
[10] Charoensirisomboon P, Inoue T, Weber M. Polymer 2000;41(4483):6907.
[11] Nair SV, Oommen Z, Thomas S. J Appl Polym Sci 2002;86:3537.
[12] Lyu SP, Cernohous JJ, Bates FS, Macosko CW. Macromolecules 1999; 32:106.
[13] Jiao J, Kramer EJ, de Vos S, Möller M, Koning C. Polymer 1999;40:3585. Jiao J, Kramer EJ, de Vos S, Möller M, Koning C. Macromolecules 1999; 32:6261.
[14] Koriyama H, Oyama HT, Ougizawa T, Inoue T, Weber M, Koch E. Polymer 1999;40:6381.
[15] Kuroda T, Torikai K, Oyama HT, Ougizawa T, Inoue T, Weber M. Kobunshi Ronbunshu 1999;56:860.
[16] Schulze JS, Cernohous JJ, Hirao A, Lodge TP, Macosko CW. Macromolecules 2000;33:1191.
[17] Oyama HT, Ougizawa T, Inoue T, Weber M, Tamaru K. Macromolecules 2001;34:7017.
[18] Schulze JS, Moon B, Lodge TP, Macosko CW. Macromolecules 2001;34: 200.
[19] Oyama HT, Inoue T. Macromolecules 2001;34:3331.
[20] Yin Z, Koulic C, Pagnoulle C, Jérôme R. Langmuir 2003;19:453.
[21] Jeon HK, Macosko CW, Moon B, Hoye TR, Yin Z. Macromolecules 2004;37:2563.
[22] Kim BJ, Kang H, Char K, Katsov K, Fredrickson GH, Kramer EJ. Macromolecules 2005;38:6106.
[23] Zhang J, Lodge TP, Macosko CW. Macromolecules 2005;38:6586.
[24] Kim HY, Ryu DY, Jeong U, Kho DH, Kim JK. Macromol Rapid Commun 2005;26:1428.
[25] Guegan P, Macosko CW, Ishizone T, Hirao A, Nakahama S. Macromolecules 1994;27:4993.
[26] Orr CA, Cernohous JJ, Guegan P, Hirao A, Jeon HK, Macosko CW. Polymer 2001;42:8171.
[27] Macosko CW, Jeon HK, Hoye TR. Prog Polym Sci 2005;30:939.
[28] Kim HY, Jeong U, Kim JK. Macromolecules 2003;36:1594.
[29] Kim JK, Lee H. Polymer 1996;37:305.
[30] Jeon HK, Kim JK. Macromolecules 1998;31:9273.
[31] Jeon HK, Kim JK. Polymer 1998;39:6227. Jeon HK, Kim JK. Korea Polym J 1999;7:124.
[32] Jeon HK, O HT, Kim JK. Polymer 2001;42:3259.
[33] Jeon HK, Kim JK. Macromolecules 2000;33:8200.
[34] Heitmiller RF, Naar RZ, Zabusky HH. J Appl Polym Sci 1964;8:873.
[35] Zhao J, Mascia L, Nassehi V. Adv Polym Technol 1997;16:209.
[36] Yu X, Wu Y, Li B, Han Y. Polymer 2005;46:3337.
[37] Kim JK, Han CD. Polym Eng Sci 1991;31:258.